

GSIV serine/threonine kinase can induce apoptotic cell death via p53 and pro-apoptotic gene Bax upregulation in fish cells

Latif Reshi^{1,2} · Horng-Cherng Wu³ · Jen-Leih Wu⁴ · Hao-Ven Wang² · Jiann-Ruey Hong¹

Published online: 30 January 2016
© Springer Science+Business Media New York 2016

Abstract Previous studies have shown that GSIV induces apoptotic cell death through upregulation of the pro-apoptotic genes Bax and Bak in Grouper fin cells (GF-1 cells). However, the role of viral genome-encoded protein(s) in this death process remains unknown. In this study, we demonstrated that the Giant seaperch iridovirus (GSIV) genome encoded a serine/threonine kinase (ST kinase) protein, and induced apoptotic cell death via a p53-mediated Bax upregulation approach and a downregulation of Bcl-2 in fish cells. The ST kinase expression profile was identified through Western blot analyses, which indicated that expression started at day 1 h post-infection (PI), increased up to day 3, and then decreased by day 5 PI. This profile indicated the role of ST kinase expression during the early and middle phases of viral replication. We then cloned the ST kinase gene and tested its function in fish cells. The ST kinase was transiently expressed and used to investigate possible novel protein functions. The transient expression of ST kinase in GF-1 cells resulted in apoptotic

cell features, as revealed with Terminal deoxynucleotidyl transferase biotin-dUTP nick-end labeling (TUNEL) assays and Hoechst 33258 staining at 24 h (37 %) and 48 h post-transfection (PT) (49 %). Then, through studies on the mechanism of cell death, we found that ST kinase overexpression could upregulate the anti-stress gene p53 and the pro-apoptotic gene Bax at 48 h PT. Interestingly, this upregulation of p53 and Bax also correlated to alterations in the mitochondria function that induced loss of mitochondrial membrane potential (MMP) and activated the initiator caspase-9 and the effector caspase-3 in the downstream. Moreover, when the p53-dependent transcriptional downstream gene was blocked by a specific transcriptional inhibitor, it was found that pifithrin- α not only reduced Bax expression, but also averted cell death in GF-1 cells during the ST kinase overexpression. Taken altogether, these results suggested that aquatic GSIV ST kinase could induce apoptosis via upregulation of p53 and Bax expression, resulting in mitochondrial disruption, which activated a downstream caspases-mediated cell death pathway.

✉ Jiann-Ruey Hong
jrhong@mail.ncku.edu.tw

¹ Laboratory of Molecular Virology and Biotechnology, Institute of Biotechnology, Department of Biotechnology and Bioindustry Sciences, National Cheng Kung University, No 1, University Road, Tainan City 701, Taiwan, ROC

² Department of Life Sciences, College of Bioscience and Biotechnology, National Cheng Kung University, No. 1, University Road, Tainan City 701, Taiwan, ROC

³ Laboratory Department of Food Science and Technology, Chin Nan University of Pharmacy and Science, Tainan 717, Taiwan, ROC

⁴ Laboratory of Marine Molecular Biology and Biotechnology, Institute of Cellular and Organismic Biology, Academia Sinica, Nankang, Taipei 115, Taiwan, ROC

Keywords Grouper sea perch virus · Serine/threonine kinase · Bax · p53 · Mitochondrial membrane potential loss · Upregulation

Introduction

A variety of DNA and RNA viruses actively induce programmed cell death (PCD) during infections, and PCD has been considered to play a critical role in the pathogenesis of viral diseases [1]. The iridovirus belongs to a large dsDNA virus family that displays icosahedral symmetry with a 120–200 nm diameter. This virus has caused a

serious decline in the global population of amphibians and heavy economic losses in the aquaculture industry [2]. A growing number of reports have demonstrated that iridoviruses can infect both invertebrates and lower vertebrates, including crustaceans, mollusks, insects, fish, amphibians and reptiles [3]. The family *Iridoviridae* is currently composed of five genera: *Ranavirus*, *Lymphocystivirus*, *Megalocytivirus*, *Iridovirus* and *Chloriridovirus* [4]. The megalocytiviruses infect a wide range of tropical marine and freshwater fish, including grouper, gourami, cichlid, red sea bream, angel fish, sea bass and lamp eye, causing similar diseases in each species. During such infections in host fish *Megalocytivirus* is found (sometimes in large numbers) in the spleen, kidney and gastrointestinal tract, and to a lesser extent in the liver, heart, gills and connective tissues [5]. The forms of cell death evoked by iridoviruses are continually being disclosed, and they include typical apoptosis and non-apoptotic cell death [6–8]. However, the signaling pathways involved in these processes remain largely unknown.

Various outbreaks of iridovirus disease have been reported in Taiwan among cultured marine fish [9–11]. The phylogenetic relationships between Taiwan isolates and those from other geographic areas are still unclear. Recent evidence shows that GSIV K1 [12] infection can induce host cell death, and it displays several features of apoptotic and post-apoptotic necrosis. The GSIV-induced apoptosis was accompanied by increased annexin V-binding to the plasma membrane, with dramatic changes in PS distribution at early mid-apoptotic GF-1 cells. Then, PS exposure on the outer leaflet of the plasma membrane occurred rapidly, with development of bulb-like vesicles as a PI-positive cell. Several potent drugs (such as the protein synthesis inhibitor CHX) can block the death process, which suggests that the death factors are involved in this pathway [12, 13]. Studying the mechanisms and physiologic functions of cell death during such virus infections can contribute to a better understanding of the host–pathogen interactions and the disease pathogenesis, which could lead to new therapeutic strategies for dealing with infectious diseases [14–17]. Therefore, a detailed elucidation of the mechanism for GSIV infection-evoked cell death is urgently needed.

The individual cells of multicellular organisms undergo systematic self-destruction through apoptosis in response to a wide variety of stimuli [18]. Therefore, apoptosis plays a central role in the normal development and homeostasis of multicellular organisms [19]. The process of PCD is controlled by a range of cell signaling pathways that originate either from the cell's external environment (extrinsic) or from within the cell itself (intrinsic) [20]. Apoptosis may be used by the host to limit the production of viruses or to disseminate them [21, 22]. However, viruses use the

apoptosis process to produce sufficient virus progeny or to facilitate virus release [21, 22].

Different molecular and biochemical tools have been identified and used to elucidate the mechanisms of PCD. However the intracellular signaling pathways that are triggered by virus infection-induced apoptotic PCD remain largely unknown. Although not all of the signals that initiate the apoptosis pathway are understood, in many (but not all) cases, the tumor suppressor protein p53 is required to propagate the signal to commit suicide [23]. The cell's fate to undergo apoptosis depends mainly on the dynamic balance between the Bcl-2 family sensor proteins, which both promote and inhibit apoptosis. Members of the Bcl-2 family of sensor proteins (such as Bax, Bad, Bid, Bak Bcl2 or Bcl-xl) represent key points in the apoptotic pathways. These proteins appear to sit at nodes in the apoptotic pathways, at points of integration for stimuli that provoke apoptosis. In many (but not all) cases, these proteins appear to influence the activation of caspase family members (proteases), which perform the “execution” phase of apoptosis by cleaving a number of cellular proteins and bringing about the destruction of cellular structures [24–26].

Mitochondrial membrane permeabilization can alter both the inner and outer mitochondria membranes, and these changes can precede the signs of necrotic or apoptotic cell death and the activation of apoptosis-specific caspases [27–29]. Many proteins from the Bcl-2/Bax family regulate apoptosis when they are present in the mitochondrial membrane. Close homologues of Bcl-2, including Bcl-xL, Bcl-W, Mcl-1 and A1, reside in the mitochondria, and they serve to stabilize the barrier function of the mitochondrial membranes [15, 30]. Pro-apoptotic proteins can shuttle between mitochondrial and non-mitochondrial localizations, functioning as the cytosols for Bax, Bad and Bid. These proteins are inserted into the mitochondrial membranes upon apoptosis induction, resulting in permeabilization [31, 32].

We recently reported that GSIV infection induces host cell apoptosis through the upregulation of the pro-apoptotic death genes Bax and Bak at the middle replication stage, and that factors in the grouper fin cell line (GF-1) have been shown to modulate this process. In studying the mechanism of cell death, we found that the upregulated, de novo-synthesized Bax and Bak proteins formed heterodimers. This upregulation process correlated with mitochondrial membrane potential (MMP) loss, increased caspase-3 activity and increased apoptotic cell death [12, 13]. In this study, we showed that GSIV-ST kinase induces apoptotic cell death via a p53-mediated upregulation of Bax which causes a loss of MMP. This loss then mediates cell death signaling, which results in an activation of the caspase-mediated cell death pathway at the mid-to-late stages of viral replication. These findings may provide new insight into GSIV-induced pathogenesis.

Materials and methods

Chemicals, drugs and antibodies used

With a RT-PCR system kit (Thermo Scientific), transfections were carried out using Lipofectamine 2000 (Invitrogen) for plasmids, according to the manufacturer's instructions. The experiments required use of a TUNEL assay kit (Roche), paraformaldehyde (4 %), Triton X, MMP loss JC-1 lipophilic dye, Hoechst nuclear stain, 3 μ m H₂O₂, Trizol reagent (BioLine) and pifithrin- α (Sigma). The following antibodies were used: anti-rabbit Bax (Cell Signaling), anti-Bcl-2, anti-mouse serine 46 p53 (Cell Signaling), anti-rabbit p53 (GeneTex), anti-EGFP, anti-kinase (recombinant protein), anti-mouse actin (Millipore), anti-mouse caspase-3 (Calbiochem) and anti-mouse caspase-9 (Cell Signaling).

Drug treatment

Pifithrin- α (PFT- α) was purchased from Sigma Aldrich, Inc. In experiments designed to study the selective blocking of p53 transcription, the cells were pre-treated with PFT- α for 5 h, followed by performance of a transient transfection assay with vector control plasmid and kinase plasmids.

Cell culture and virus

Grouper fin cells (GF-1 cells) were provided by Dr. Chi (Institute of Zoology and Development of Life Sciences). The cells were maintained under standard conditions (at 28 °C) in Leibovitz's L-15 medium, supplemented by 5 % fetal bovine serum (FBS) and 25 μ g/ml of gentamycin antibiotic. The cells were passaged twice weekly. All experiments were performed with cells in the logarithmic growth phase. Naturally infected giant sea perch were collected in 2005 in the Kaohsiung Prefecture, and these fish were the source of the GSIV Kaohsiung No. 1 (GSIV K1) strain that was used to infect the GF-1 cells used in this study. GSIV-K1 is an RSIV-like strain (Accession number: KT804738), with a comparable major capsid protein [12]. The virus was purified and stored at -80 °C until use. The viral titer was determined by using the median tissue culture infective dose (TCID₅₀) assay, in accordance with the method developed by Dobos et al. [33].

RNA isolation and RT-PCR cloning and sequence analysis of GSIV ST kinase

RNA was extracted using the Trizol reagent from stable GSIV-K1 infected GF-1 cells. RNA samples were subjected to reverse transcriptase, using an RT-PCR kit according to the manufacturer's instructions, with (0.5 μ g

oligo (dT) primers for the first strand synthesis to generate cDNA libraries. The cDNA then were subjected to standard PCR, using the upstream primer GTGTAACCA/TATGTT TACTCAATTGCCGCAC and the downstream primer TCCGC/TCGAGCGACCGCATTGAAGGCAC to amplify a kinase gene fragment. The PCR cycling conditions were 94 °C for 5 min, 94 °C for 30 s., 60 °C for 30 s., 30 to 35 cycles, 72 °C for 30 s and 72 °C for 7 min. As an internal control, an actin cDNA fragment was amplified using an upstream primer and a downstream primer [15]. The purity and size of the amplified product was confirmed with 1.2 % agarose gel electrophoresis after ethidium bromide staining. The double-stranded cDNA product (1430 bp) was purified by using the QIAquick™ gel extraction system (Qiagen, Valencia, CA, USA), and was sub-cloned with the pGEM-T easy cloning system (Promega, Madison, WI, USA). Cloned PCR products were sequenced by the dye termination method using an ABI PRISM 477 DNA sequencer (PE Biosystems, Foster City, CA, USA), and were scanned against the GenBank database BLAST (www.genome.jp/tools/blast/) and the SBASE domain prediction system (www.icgeb.trieste.it/sbase/) programs.

ST kinase-enhanced green fluorescent protein (EGFP) gene fusion constructions

The ST kinase coding sequence from GSIV (kinase cDNA in pGEM-T-easy plasmid) was amplified by using the sense primer 5'-GAAGATCTATGTTTACTCAATTGCCGC AC-3' (the BgIII I site is underlined, and the start codon of the kinase is in boldface) and the anti-sense primer 5'-GC GGATCCTCACGACCGCATTGAAGGCAC T-3' (the BamHI site is underlined). This amplification produced the kinase-EGFP fusion genes to monitor the kinase-induced cellular morphological changes (see Table 1) [15]. The PCR products were ligated with the predigested pEGFP (enhanced green fluorescent protein)-N3 vector (BD Biosciences, Clontech, Palo Alto, CA, USA) after the restriction digestion with Xho I and BamHI to create pEGFP-ST kinase. Cell transfection was implemented by seeding 3×10^5 GF-1 cells in 60 mm culture dishes one day prior to the transfection. The following day, pEGFP or pEGFP-ST kinase (2 μ g) was added to the cells, using Lipofectamine 2000 (Invitrogen). Expression of the EGFP fusion proteins was detected visually by using a fluorescence microscope with an FITC filter. The numbers of EGFP or EGFP-ST kinase-containing apoptotic cells (among 200 cells per sample) were assessed in three individual experiments. Each point represented the mean EGFP or EGFP-ST kinase-containing apoptotic cells of three independent experiments \pm the standard error of the mean (SEM). The data were analyzed using either the paired or unpaired Student's *t* test, as was appropriate. The statistical

Table 1 The sequence primers used in this study

Name		Primers
pET-29a(+)-ST kinase	Forward	GTGTAACCA/TATGTTTACTCAATTGCCGCAC (NdeI)
	Reverse	TCCGC/TCGAGCGACCCGATTGAAGGCAC (XhoI)
pEGFP-C1-ST kinase	Forward 1	GAAGATCTATGTTTACTCAATTGCCGCAC (Bgl II)
	Forward 2	GAGAATTCTATGTTTACTCAATTGCCGCAC (EcoRI)
	Reverse 1	GCGGATCCTCACGACCCGATTGAAGGCAC (BamHI)

The enzymatic cutting sites on nucleotides of primers are underlined

significance between the mean group values was defined as a *p* value <0.05.

TUNEL assay

The DNA fragmentation was further analyzed with a DNA fragmentation assay kit (Roche, CA, USA), according to the manufacturer's recommendations. To summarize the process, the GF-1 cells were seeded onto 24-well plates at a concentration of 3×10^5 cells per well 1 days prior to the transfection procedure, and 2 µg of EGFP and EGFP-ST kinase was added to the cells, using Lipofectamin 2000 (Life Technologies). The treatment group plates were incubated at 28 °C (GF-1 cells) for 24 and for 48 h. The cells were recovered, washed with phosphate buffered saline (PBS), and fixed with a freshly prepared paraformaldehyde solution (4 % in PBS, pH 7.4) for 30 min at room temperature. The slides were washed with PBS and incubated in blocking solution (0.3 % H₂O₂ in methanol) for 30 min at room temperature. Petri dishes were rinsed with PBS, incubated with permeabilization solution (0.1 % Triton X-100 in 0.1 % sodium citrate) for 5 min on ice, and rinsed twice with PBS. Terminal deoxynucleotidyl transferase biotin-dUTP nick-end labeling (TUNEL) reaction mixture from an in situ cell death detection kit (Boehringer-Mannheim, Mannheim, Germany) was added to the sample (50 µl), and the Petri dishes were incubated in a humidified chamber for 60 min at 37 °C. The samples were examined with fluorescence optics or phase-contrast microscopy after signal conversion. Signal conversion was performed by incubating the samples with anti-fluorescein antibody (50 µl) conjugated with horseradish peroxidase in a humidified chamber for 60 min at 37 °C and rinsed with PBS. Finally, 50–100 µl of diaminobenzidine substrate solution was added for 10 min at room temperature. Each sample was rinsed with PBS, and a glass coverslip was placed in the bottom of each dish. The samples were examined under a light microscope [8, 13].

Hoechst 33258 nuclear staining

The cells were then seeded onto 24-well plates at a concentration of 2×10^4 cells per well 1 days prior to the

transfection procedure, and 2 µg of EGFP and EGFP-ST kinase was added to the cells using Lipofectamin 2000 (Life Technologies). The treatment group plates were incubated at 28 °C (GF-1 cells) for 24 and 48 h. At various points in time after the transfection, the cells were washed, fixed and permeabilized with PBS containing 0.2 % Triton X-100-PBS for 5 min on ice. Each used well was subjected to nuclear staining with (0.5 µg/ml) of Hoechst 33258 at 38 °C for 15 min. The cells were then observed by using an Olympus fluorescence microscope (Olympus DP70, Tokyo, Japan) with a 360 nm filter for excitation and a 500 nm filter for emission [8].

Western blotting analysis

The GF-1 cells were seeded at 1×10^5 cells per ml on a 60-mm Petri dish for at least 20 h prior to cultivation. The resulting monolayers were rinsed twice with PBS, after which the cells were infected with virus at a MOI of 1, and then incubated for 0, 1, 3 or 5 days. The pEGFP, pEGFP-ST kinase and plasmids were added to the cells (2 µg each) after 20 h, using Lipofectamine-Plus (Life Technologies). Transfection was allowed to proceed for 5.5 h. The GF-1 cells were incubated at 28 °C for 0, 24 and 48 h. The culture media were aspirated at the end of each time point, after which the cells were washed with PBS and lysed in 0.3 ml lysis buffer (10 mM Tris base, 20 % glycerol, 10 mM sodium dodecyl sulfate and 2 % β-mercaptoethanol; pH 6.8). Proteins were separated by sodium dodecyl sulfate polyacrylamide gel electrophoresis, electro blotted and then subjected to immunodetection, as previously described. The membranes were incubated with a dilution of anti-GSIV-MCP polyclonal mouse antibodies (1:5000, home-made), anti-GSIV-kinase polyclonal rabbit mouse (1:1000, home-made), anti-mouse Bax MAb (1:1000; BD Biosciences, San Jose, CA, USA), anti-mouse Bcl-2 antibody (BD Biosciences), anti-mouse caspase-3 MAb (1:1000, BD Biosciences), anti-mouse caspase-9, anti-mouse β-actin MAb (1:2500; Chemicon, Temecula, CA, USA), anti-mouse EGFP MAb (1:10,000, Clontech Laboratories, Mountain View, CA, USA), and a dilution of an appropriate secondary antibody (1:7500 to 1:10,000)

that included peroxidase-labeled goat anti-mouse (Amersham, Piscataway, NJ, USA) and goat anti-rabbit (Amersham) antibodies. Chemiluminescence detection was performed using a Western Exposure Chemiluminescence Kit (Amersham), according to the manufacturer's instructions. The chemoluminescence indication of antibody binding was captured by Top Bio Multigel-21 (Total Lab Systems TLS) [15].

Evaluation of mitochondrial membrane potential (MMP) with a lipophilic cationic dye

The changes in MMP that occurred during the apoptosis induced by the ST kinase gene of the GSIV virus were examined by using a JC-1 Mito-ID membrane potential aggregation dye. The GF-1 cells were seeded onto 24-well plates at concentrations of 2×10^4 cells per well, 1 days prior to the transfection procedure, and 2 μ g of EYFP and EYFP-ST kinase plasmids were added to cells by using Lipofectamin 2000 (Life Technologies). The treatment group plates were incubated at 28 °C (GF-1 cells) for 24 and 48 h. At various points in time after transfection, the cells were washed, fixed and permeabilized with PBS containing 0.2 % Triton X-100-PBS for 5 min on ice. After 24 and 48 hpt, both the transfected cells and the non-transfected cells (treated with H₂O₂ as a positive control) were rinsed in 1 % PBS and incubated with Mito-id JC-1 dye for 30 min at 28 °C. The cells were then washed with PBS, suspended in LB medium and analyzed by fluorescence microscopy [13].

Cell counts

The numbers of TdT-dUTP-labeled nuclei or TUNEL-positive cells in were counted in each sample of 200 cells. The results were all expressed as mean \pm SEM. The data were analyzed using either paired or unpaired Student's *t* tests, as appropriate. A value of $p < 0.05$ was taken to represent a statistically significant difference between the group mean values.

Results

GSIV ST kinase gene expression profile and cloning

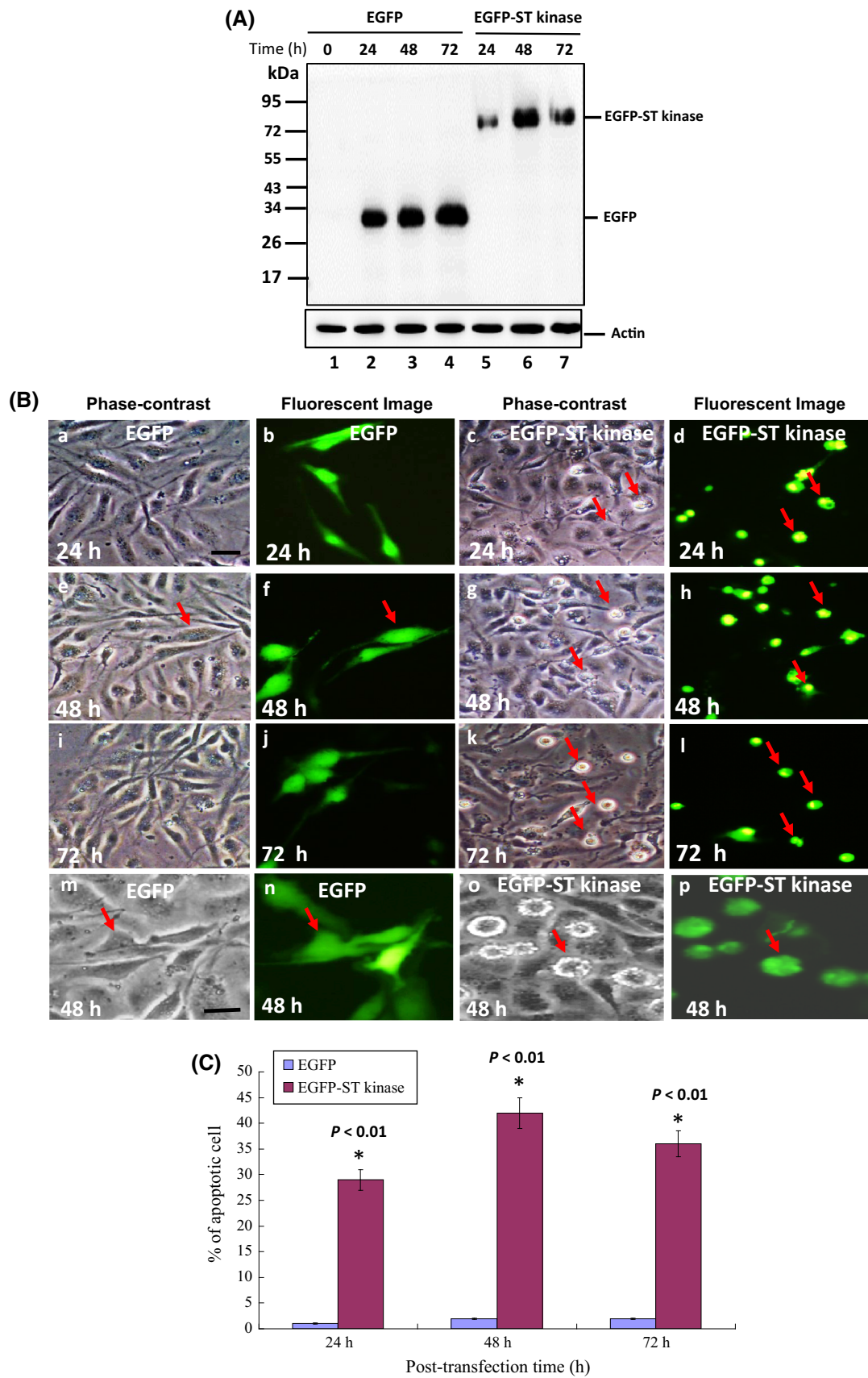
The GSIV ST kinase expression profile was identified, as shown in Fig. 1a. The gene quickly expressed at day 1 and continued to express at days 3 and 5, which seemed to show the behavior of an early expression gene. Then we cloned this gene and tried to analyze its function. The full length of the GSIV ST kinase included 1430 base pairs for encoding a 465 amino acid protein that had an approximate

Fig. 2 GSIV ST kinase directly induces apoptotic cell death in GF-1 cells. **A** Western blot analysis of EGFP and ST kinase-EGFP proteins in GF-1 cells following transfection and incubation for 0 h (lane 1) as a control, 24 h (lane 2), 48 h (lane 3), 72 h (lane 4), 24 h (lane 5), 48 h (lane 6) and 72 h (lane 7). ST kinase-EGFP and EGFP proteins were detected by Western blot analysis; the gels were immunoblotted with a monoclonal antibody to EGFP. **b**: β -actin as an internal control. **B** Phase-contrast micrographs of transfected and untransfected apoptotic GF-1 cells at different time points (24, 48 and 72 h). Phase-contrast micrographs of EGFP [*a* (24 h), *e* (48 h), *i* (72 h) and *m* (48 h) at high magnification]; phase-contrast and fluorescent images [*b* (24 h), *f* (48 h), *j* (72 h) and *n* (48 h) at high magnification] and phase-contrast micrographs of ST kinase-EGFP [*c* (24 h), *g* (48 h), *k* (72 h) and *o* (48 h) at high magnification]; phase-contrast and fluorescent images [*d* (24 h), *h* (48 h), *l* (72 h) and *p* (48 h)], in which rounded-up and plasma membrane blebbing cells are indicated by arrows. **C** The percentage of apoptotic EGFP and ST kinase-EGFP-transfected cells at different time points. The numbers of EGFP- or ST kinase-EGFP-containing apoptotic cells in each 200 cell sample were assessed in three individual experiments. Each point represented the mean EGFP or ST kinase-EGFP-containing apoptotic cells of three independent experiments \pm the standard error of the mean (SEM). The data were analyzed using either paired or unpaired Student's *t* tests, as appropriate. Statistical significance was defined as p values < 0.05

molecular weight of 51.2 kDa (Fig. 1b). When the amino acid identity of the serine/threonine kinase (ST kinase) from the GSIV-K1 strain (Accession number: KT804738) was compared with that of other species, a 99 % match was found for OSGIV (B; [AY894343.1](#)), a 99 % match for the RBIV-C1 (C; [AGG37893.1](#)), a 99 % match for RBIV-KOR-TY1 (D; [AAT71828.1](#)), a 97 % match for RSIV (E; [AB104413.1](#)), a 92 % match for TRBIV (F; [ADE34358.1](#)) and a 90 % match for ISKNV (G; [AF371960.1](#)). These results indicated an evolution tree, as shown in Fig. 1c, which is based on sequence identity. Furthermore, as shown in Fig. 1d, the possible prediction protein modification sites in the protein kinase were as follows: (1) an Acyl-CoA dehydrogenase-like domain (16–42 aa); (2) a protein kinase-like domain (73–181 aa); (3) a DNA polymerase B region-like domain (219–299 aa) and (4) an auxin efflux carrier-like domain (372–419 aa). All of these sites could have been playing multifunctional roles.

Overexpression of GSIV ST kinase induces apoptosis, or cell death

Kinase was fused with EGFP, and the resulting fusion gene was used to directly monitor the ST kinase-induced cell morphological changes. The expression of approximately 84 kDa EGFP-ST kinase fusion protein was detected at 24, 48 h and 72 hpt by using the Western blot method (Fig. 2A), compared with an expression of 32 kDa from EGFP alone. To monitor the cellular morphological changes such as cell rounding up and plasma membrane blebs, we created a serine



threonine kinase-EGFP expression plasmid. Examination of the serine threonine protein kinase expression profile in fish GF-1 cells revealed the gradual expression of ST kinase-EGFP (Fig. 2A, panel a, lanes 5–7) compared to that of the EGFP control group (Fig. 2A, panel b, lanes 2–4). ST kinase-EGFP induced GF-1 cell death (Fig. 2B, C). Specifically, GF-1–ST kinase EGFP expression was associated with cell rounding and the formation of membrane blebs at 24 hpt (Fig. 2B, panels c and d). No such observations were noted in cells expressing EGFP-control (Fig. 2B, panels a and b). ST kinase-EGFP gradually induced cell death through apoptosis (arrows) from 24 h (28 %, Fig. 2B, panels c and d), 48 h (42 %, Fig. 2B, panels g and h) and 72 h (36 %, Fig. 2B, panels k and l), as compared to the EGFP-control groups at 24 h (1 %, Fig. 2B, panels a and b), 48 h (2 %, Fig. 2B, panels e and f) and 72 h (3.5 %, Fig. 2B, panels i and j). These observations corresponded to the determined apoptosis ratios (Fig. 2C).

Next, to confirm the nuclear structure by Hoechst 33254 staining, we examined GF-1 cells for another characteristic

phenotypic that is associated with apoptosis, namely chromatin condensation and breakdown of nuclear material. The GF-1 cells were transfected with EGFP and EGFP ST kinase plasmid. The cells that were transfected with EGFP plasmid alone (Fig. 3a–f) showed uniform staining of the nuclei. However, the ST kinase plasmid transfected cells showed fragmented nuclei, with condensed chromatin or multiple apoptotic bodies (Fig. 3g–l). These effects were especially clear at 72 hpt (Fig. 3i and l; indicated by arrows).

Next, TUNEL assays established that cells in which ST kinase-EGFP was produced underwent apoptosis at between 0 h and 48 hpt. As shown in Fig. 4A, (panel A, g and i, at 24 h and 48 hpt) displayed more apoptotic observations (see arrows) in the GF-1 cells than the EGFP control group (panel A, a and c, at 24 hpt and b at 48 h). The percentage of TUNEL-positive cells induced by ST kinase-EGFP (Fig. 4B) increased with time (37 % at 24 h and 49 % at 48 h), compared to the negative controls (1 % at 24 h and 2.5 % at 48 h). This difference, therefore, was significant.

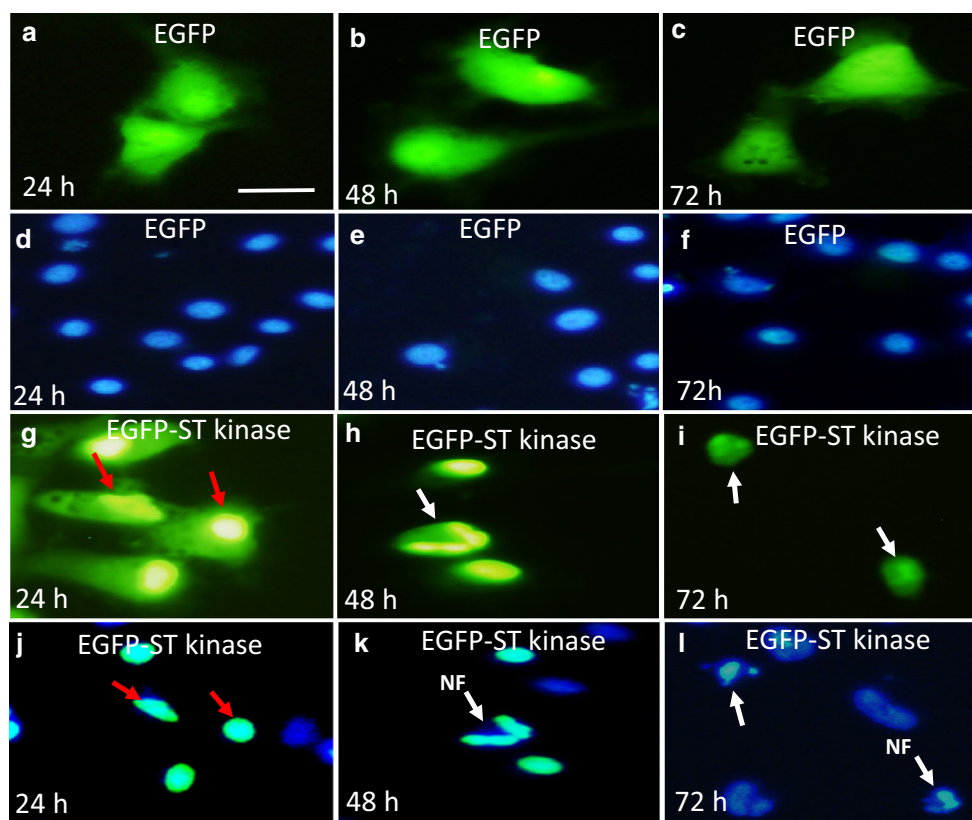


Fig. 3 Identification of nuclear condensation and nuclear fragmentation upon transfection of GSIV ST kinase gene into GF-1 cells. Control EYFP GF-1 cells (*horizontal-upper panel 1* (a, b and c) for *green fluorescence* images; panel 2 (d, e and f) for Hoechst 33254 staining images at 24, 48 h and 72 hpt. The ST kinase-expressing GF-1 cells (*lower panel 1*) (g, h and i) for *green fluorescence* images; panel 2 (j, k and l) for Hoechst 33254 staining images at 24, 48 h and

72 hpt. The cells were grown in medium supplemented with 5% calf serum. After 20 h, the cells were transfected with ST kinase plasmid attached with EGFP as a reporter gene. After 24 and 48 h, the cells were stained with Hoechst 33258. Nuclear condensation and fragmentation are evident with GF-1 cells that are indicated by arrows. Scale = 10 μ m. *N* nucleus, *NC* nuclear condensation, *NF* nuclear fragmentation (Color figure online)

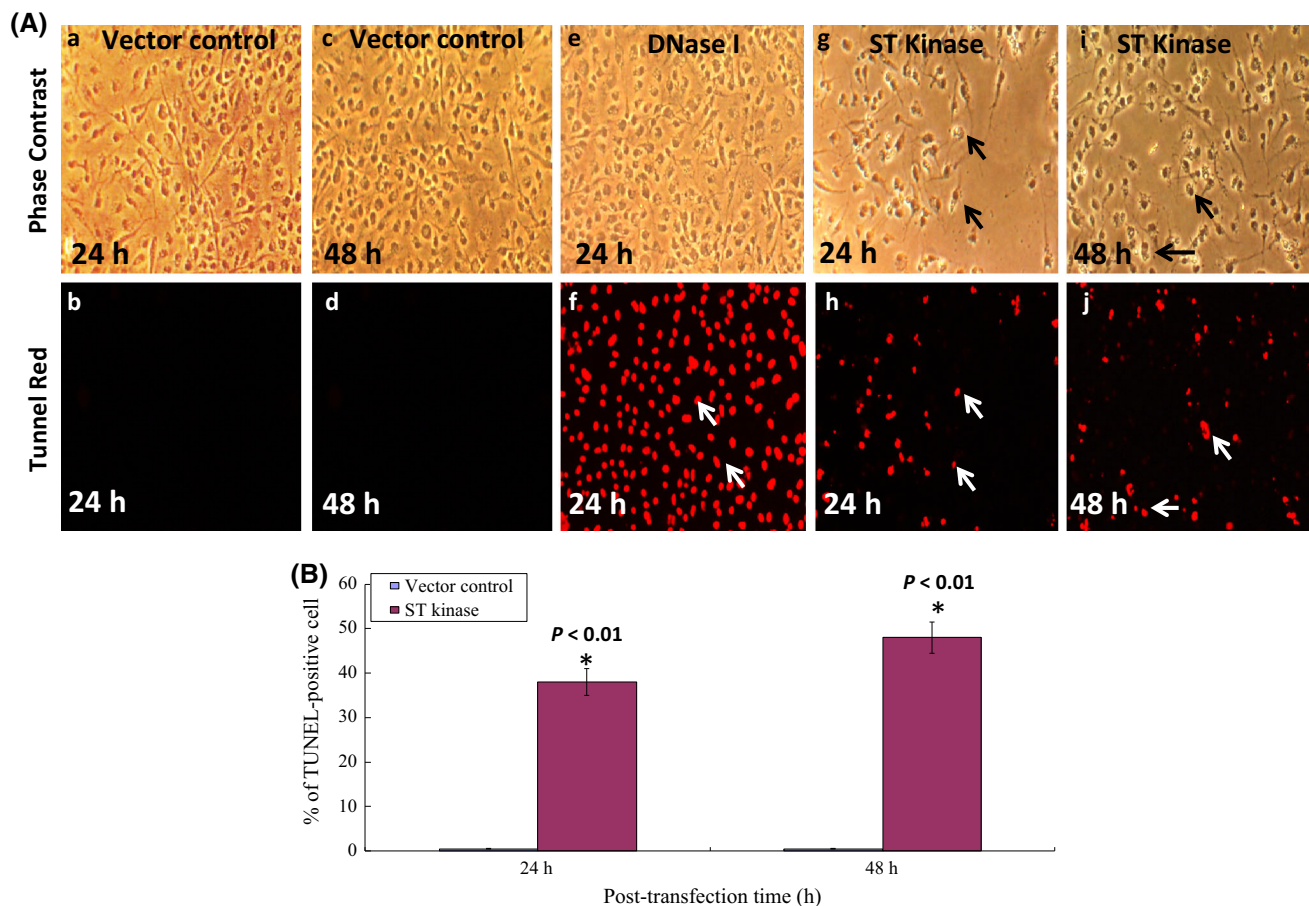


Fig. 4 GSIV ST kinase expression can induce apoptotic cell death in GF-1 cells, as shown by TUNEL assays. **(A)** The cells were transfected with ST kinase gene and analyzed at 24 h and 48 hpt by using fluorescently labeled anti-BrdU antibodies. The levels of fluorescence were detected under a microscope. The *upper panel* (a, c, e, g, i) shows cells visualized under visible light without a filter; the *lower panel* (b, d, f, h, j) shows cells visualized under specific filters for fluorescence detection. The *upper and the lower panels* show cells under the same microscopic fields. a and c: cells were transfected with control plasmid pcDNA 3.0 (–) vector at 24 and 48 h. Untransfected control cells (e) were treated with DNase as

positive control. The g and i cells were transfected with pcDNA3-ST kinase construct in g and i at 24 h and 48 hpt, respectively. **(B)** The percentage of apoptotic-positive number cells during ST kinase expression in GF-1 cells. The numbers of TUNEL-positive cells among samples of 200 cells were assessed in three individual experiments. *Each point* represents the mean TUNEL-positive cells of three independent experiments \pm the standard error of the mean (SEM). The data were analyzed using either paired or unpaired Student's *t* tests, as appropriate. Statistical significance was defined as *p* values <0.05

Overexpression of GSIV ST kinase upregulate p53, Bax and downregulate Bcl-2 protein in GF-1 cells

To study the molecular mechanism involved, we next identified genes that were upregulated and involved in the ST kinase-induced molecular cell death pathway. During this screening, upstream events showed increased involvement in the upregulation of p53 at 24 h (by 1.6 times, Fig. 1A: lane 5) and at 48 h pt (by 2.5 times, Fig. 5a: lane 6), compared with the effects at day zero (Fig. 5a, lane 4). Downstream events showed that the upregulation expression of the pro-apoptotic protein Bax was elevated following the ST kinase-EGFP transfection of GF-1 cells (Fig. 5a). Bax expression was elevated at 24 h (by 2.0

times, Fig. 5a: lane 5) and at 48 h (by 2.1 times, Fig. 5a: lane 6) compared to that of the ST kinase-EGFP-transfected cells at 0 h (lane 4), which displayed very little Bax background expression upon kinase overexpression compared to the negative control EGFP-transfected cells. The positive control (MCF 7) is shown in Fig. 5a, lane 7. The expressed levels were measured, as shown in Fig. 5b and 5c, in which the levels of either p53 or Bax are shown to be significantly different.

In contrast, the expression of Bcl-2 was apparently reduced upon ST kinase-EGFP expression at 24 h (by 0.7 times; Fig. 6: lane 5) and at 48 hpt (by 0.5 times; Fig. 6: lane 6) as compared with the levels of expression at 0 h (no change; Fig. 6: lane 4) and in the negative control EGFP

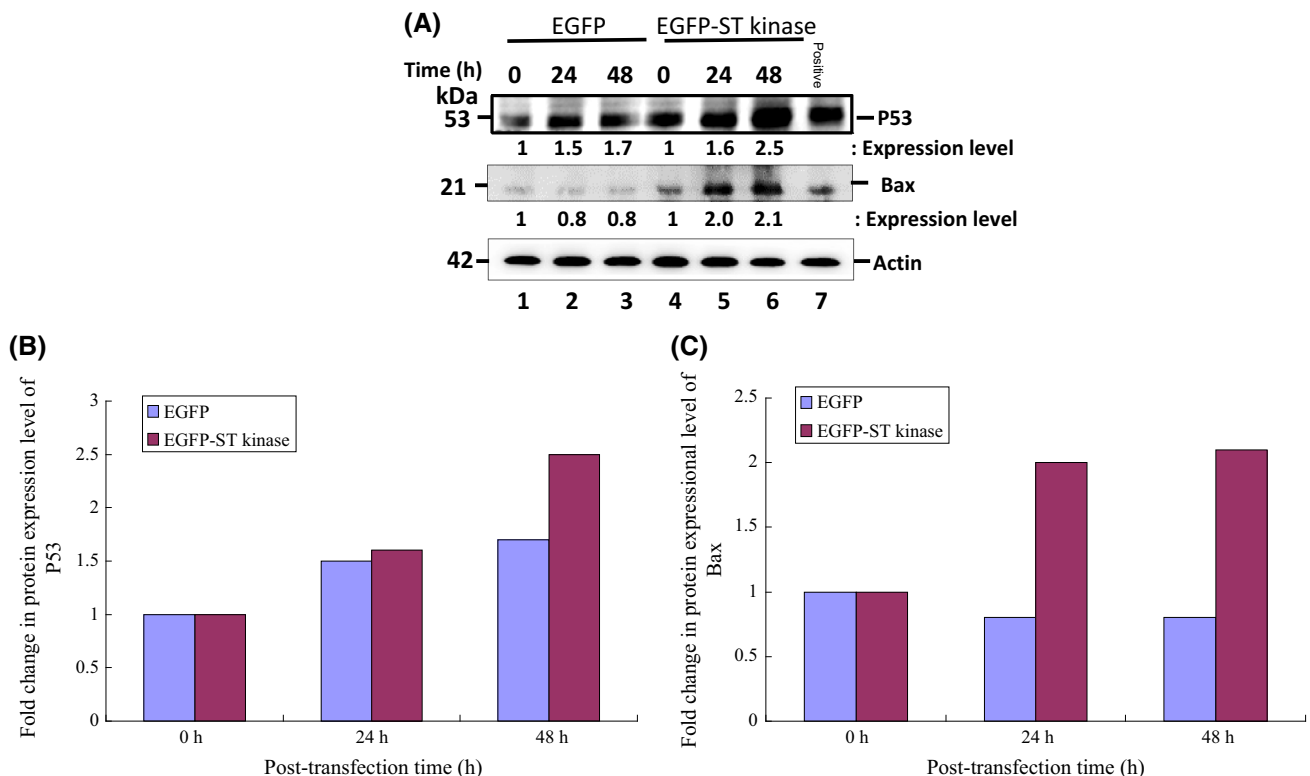


Fig. 5 GSIV ST kinase expression can upregulate *p53* and *Bax* gene in GF-1 fish cells. **a** Identification of *p53* and *Bax* proteins by Western blot analysis. Transfection of GF-1 cells with control and ST kinase plasmid at 0, 24 h and 48 hpt in GF-1 cells, where lanes 1–3 display transfected pCDNA3.1 plasmid; lanes 4–6 display transfected pCDNA3.1-ST kinase plasmid; and lane 7 shows the control MCF-

7 cell lysate. Blots were probed with an anti-mouse *p53* and *Bax* monoclonal antibody (1:7500), an anti-human *Bcl-2* monoclonal antibody (1:1000) and an anti-mouse actin monoclonal antibody (1:12500). **(b** and **c**) Quantification of protein expression level by Image J software, from **a**

alone group (Fig. 6: lanes 1–3). The levels of expression were measured, and Fig. 6b shows that they were significantly different.

ST kinase overexpression can induce MMP loss in GF-1 cells

To determine whether ST kinase expression induced an MMP loss in the downstream death pathway in fish cells, the expression levels of ST kinase and EGFP alone were examined by Western blot analysis at 24 and 48 h, as shown in Fig. 2A. Then, JC-1 dye staining was used to monitor MMP loss during the ST kinase expression. The MMP loss was noted in the GF-1 cells (arrows) at 24 h (Fig. 7A: g, h and i; enlarged images s, t and u) and at 48 h (Fig. 7A: m, n and o), compared to the low levels of MMP loss (arrows) in the vector (negative) control at 24 h (Fig. 7A: d, e, f; enlarged images p, q and r) and at 48 h (Fig. 7A: j, k and l). The H_2O_2 treatment (3 μ g/ml), which served as a positive control, produced a more pronounced MMP loss in the GF-1 cells (arrows) (Fig. 7A, a, b, c). Furthermore, the proportion of ST kinase-induced MMP

loss (Fig. 7B) was elevated in the transfected cells (28.7 % at 24 h and 51.4 % at 48 h) compared to that of the normal controls (0.5 % from 0 to 48 h), which was a significant difference. The positive control (84–98 % from 24 h to 48 hpt) is not shown.

ST kinase overexpression can activate caspases cascade (–9 and –3)

ST kinase overexpression was more coincident with cleaved caspase-9 from procaspase-9, as was shown by Western analysis at 24 and 48 h pt (Fig. 8a, lanes 5 and 6,) than it was at 0 h (Fig. 8a, lane 4) or with EGFP alone at 0, 24 and 48 h (Fig. 8a, lanes 1, 2 and 3). Furthermore, we found that the conversion of pro-caspase-3 to mature caspase-3 was more pronounced upon ST kinase overexpression in GF-1 cells at 24 and 48 h PT (Fig. 8b, lanes 5 and 6) than at 0 h (Fig. 8b, lane 4) or in EGFP-transfected alone cells at 0, 24 or 48 h (Fig. 8b, lanes 1–3). These results showed a very minor background difference between the cleaved caspase-3 form and the procaspase-3 precursor form.

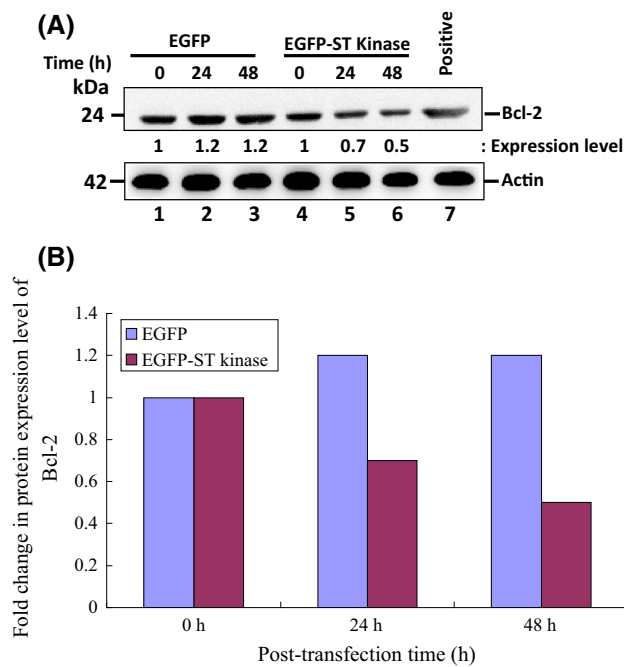


Fig. 6 The GSIV ST kinase expression downregulates the anti-apoptotic gene Bcl-2 in GF-1 fish cells. **a** Transfection of GF-1 cells with control and ST kinase plasmid at 0, 24 h and 48 hpt in GF-1 cells, where lanes 1–3 display transfected pCDNA3.1 plasmid; lanes 4–6 display transfected pCDNA3.1-ST kinase plasmid; and lane 7 contains the control MCF-7 cell lysate. Blots were probed with an anti-human Bcl-2 monoclonal antibody (1:1000) and an anti-mouse actin monoclonal antibody (1:12500). This figure is representative of the cultured cells from three separate experiments. **b** Quantification of Bcl-2 protein expression level by Image J software, from **a**

P53 activity inhibitor, pifithrin- α can reduce the ST kinase-induced cell death

We next sought to determine if treatments of the p53 activity inhibitor PFT- α could block the p53 function for averting ST kinase-induced cell death. The results indicated that PFT- α treatment could reduce kinase-induced apoptosis, according to TUNEL assay results on GF-1 cells at 24 and 48 h PT (Fig. 9A: lanes g, h and i; as indicated by arrows). These results were greater than those for the EGFP-ST kinase group (Fig. 9A: lanes d, e and f; as indicated by arrows) or for the group having EGFP alone (Fig. 9A: lanes a, b and c). Next, the TUNEL positive cell count (shown in Fig. 9B) indicated that the inhibitor treatment could reduce the cells by 10 and 24 % at 24 and 48 h pt, respectively, and that these results were significantly different than those of the without-treatment group (EGFP-ST kinase).

Furthermore, we conducted tests to determine whether the PFT- α inhibitor could block the p53-dependent transcriptional targets such as Bax after ST kinase overexpression in GF-1 cells at 48 h PT. We found that the PFT- α

treatment group could apparently reduce the downstream gene expression of Bax (Fig. 9C, lane 5) more than that of the ST kinase group (Fig. 9C, lane 4), the EGFP group (Fig. 9C, lanes 2 and 3) or the without-transfection group (Fig. 9C, lane 1). However, the PFT- α treatment group could also reduce Bcl-2 downregulation at 48 h PT (Fig. 9C, lane 5) more than the ST kinase overexpression group (Fig. 9C, lane 4). Then, the quantification of protein expression level (Fig. 9C) was counted by Image J software (as shown in Fig. 9D), which showed an up to 100 % increase of density in Bax, but reduced the anti-apoptotic factor Bcl-2 by 30 %, which was a significant difference.

Discussion

In aquatic fish, the emergence of deadly iridoviral diseases has caused a growing interest in the mechanism of iridovirus-induced host cell death [34]. Among iridoviruses, the megalocytivirus has attracted a great deal of attention since the late 1980s for its capacity to cause serious systemic diseases in a wide range of economically important freshwater and marine fish species in the Asia Pacific region [34, 35]. Despite its severe economic effects, the megalocytivirus has been insufficiently studied. In this study, we examined a novel ST kinase-like protein from the double-stranded DNA virus GSIV, and we demonstrated that the ST kinase expression triggered apoptotic cell death through upregulation of the p53 and the pro-apoptotic death factor Bax, which further induced the mitochondria-dependent cell death pathway in fish cells. Therefore, we concluded that better characterization of the GSIV molecular regulation processes could help in elucidating the mechanisms of viral pathogenesis and infection.

The GSIV ST kinase was identified as an early expression protein at day 1 after GSIV infection, and this protein continued its expression at the middle and late phases of replication. Therefore, the GSIV ST kinase may play an important role during viral replication (Fig. 1), but researchers have so far failed to define this role. Our study is the first to report on the possible function of this protein. We tried to clone and monitor this expression protein with EGFP (a variant derived from the green fluorescent protein found in the jellyfish *Aequorea victoria*) to gain a greater understanding of the protein's function.

The tracking of ST kinase localization with EGFP in GF-1 cells has revealed that proteins localize in the cytosol, and partially in the nucleus at 24 h and 48 hpt (Fig. 3). To examine this process further, it was important to monitor gene expression and fusion protein localization in vivo or in situ, and to determine the cellular morphological

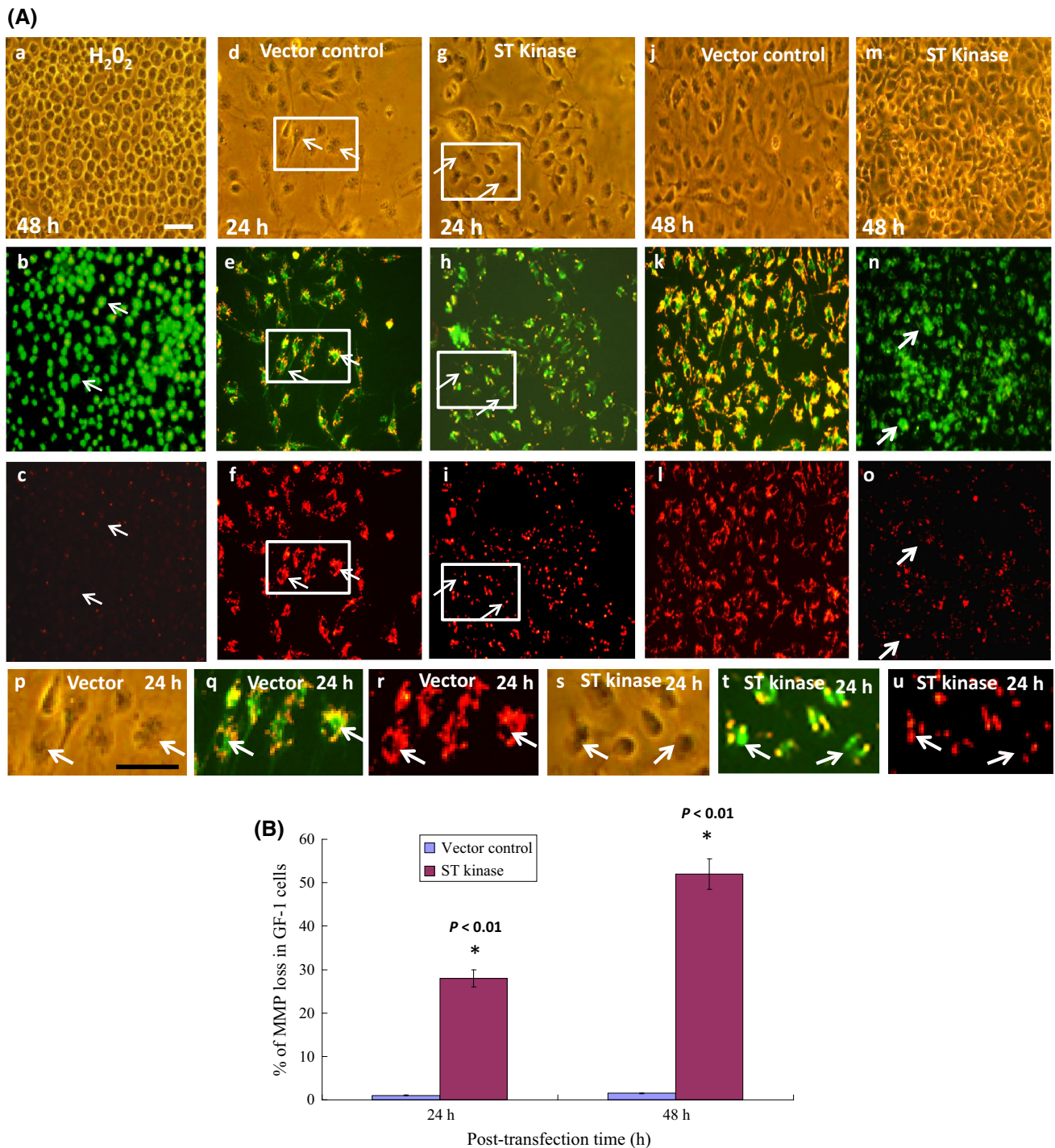


Fig. 7 GSIV ST protein kinase can induce loss of MMP in GF-1 cells. **A** Identification of ST protein kinase inducing MMP loss in GF-1 cells at 24 h and 48 hpt. Positive control cells are shown at 24 h (**A**: *a–c*; indicated by *arrows*), negative control pCDNA3.1 vector cells at 24 h (**A**: *d–f* and *p–r* for enlarged images from the *rectangular boxes*), GSIV ST kinase-transfected cells at 24 h (**A**: *g–i* and *s–u* for enlarged images from the *rectangular boxes*), with loss of MMP cells indicated by *arrows*. The negative control cells (**A**: *j–l*) and the GSIV ST kinase

(**A**: *m–o*) are shown at 48 h. Scale = 20 μ m. **(B)** The ST kinase induced losses of MMP in GF-1 cells were counted at 0, 24 h and 48 hpt. The numbers of MMP-loss cells among each of the 200-cell samples were assessed in three individual experiments. *Each point* represents the mean MMP-loss cells of three independent experiments \pm the standard error of the mean (SEM). The data were analyzed using either paired or unpaired Student's *t* tests, as appropriate. Statistical significance was defined as *p* values <0.05

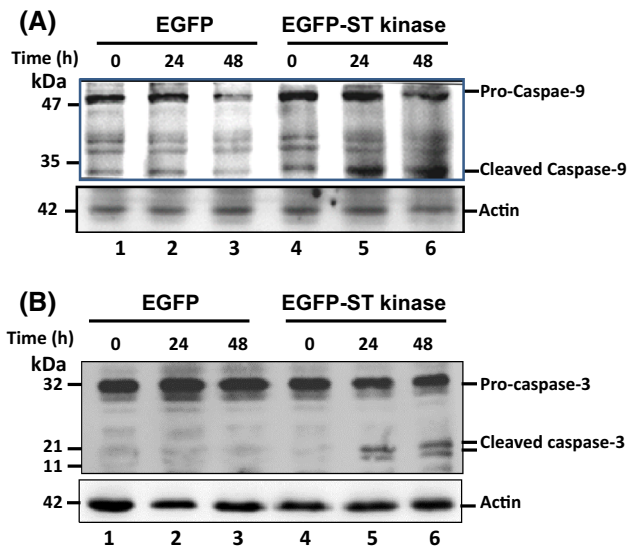


Fig. 8 GSIV ST kinase overexpression can activate caspases-9 and -3 in GF-1 cells. **(a and b)** Transfection of GF-1 cells with control and ST kinase plasmid at 0, 24 and 48 hpt in GF-1 cells that showed overexpression of ST kinase-induced caspase-9 **(a)** and caspase-3 cleavage **(b)** from procaspase-9 and procaspase-3, as determined by Western blot analyses. Lanes 1–3 correspond to EGFP-transfected cells at 0, 24 and 48 h; lanes 4–6 correspond to ST kinase-EGFP-transfected cells at 0, 24 and 48 h

changes involved [36]. We used the EGFP as a marker for the visualization of apoptotic cell morphological changes, which allowed us to trace the kinase localization, which correlated with individual protein functions. Interestingly, we found that the ST kinase expression could directly induce cell morphological changes such as cell rounding or plasma membrane blebbing (Fig. 2B).

Viruses have developed multiple strategies for manipulating the biological processes within infected cells through co-evolution with the viral host species. Viruses can regulate cell proliferation, differentiation and death [37, 38]. Meanwhile, many viruses also inhibit apoptosis, which is a strategy that subverts one of the most ancient (non-immune) anti-viral mechanisms, namely the apoptotic suppression of infected cells. Suppression of apoptosis allows viruses to replicate before the host cells die [38]. Moreover, viruses may induce apoptosis of either infected cells or of immunologically relevant cells, which can allow them to increase the viral spread or to subvert the host's immune responses [39].

There is widespread agreement that mitochondria have a function in apoptosis [40–43], but theories concerning the mechanisms involved remain controversial. The limited available data on fish cells indicate that a strain of megalocytivirus can induce apoptosis through MMP loss in a grouper liver cell line [12, 13]. Our results were consistent with these findings, as we showed a kinase induced Bax

expression in GF-1 cells (Fig. 5A) that corresponded to MMP loss (Fig. 7A).

Other viral proteins, including the human immunodeficiency virus-1 (HIV-1), Vpr protein kinase [44], the hepatitis B virus X protein [45] and the fish virus betanodavirus B2 [42, 43], also induce cell death through a mitochondria-dependent pathway, but not through Bax upregulation. In addition, the activation of caspases, as a downstream death event that participates in apoptosis, can be divided into two kinds: activation of the initiator caspases (including caspases –2, –8, –9 and –10) and activation of the effector caspases (including caspases –3, –6 and –7). Caspases are synthesized as proenzymes with very low intrinsic activity, and they require activation, either by proteolytic maturation or through interaction with an allosteric activator [17]. We found that the initiator caspase-9 and the effector caspase-3 (Fig. 8) were also activated by ST kinase expression, which could trigger a common death pathway.

The tumor suppressor p53 mediates cell apoptosis by targeting the transcriptional activities of a large number of genes [46, 47]. In addition to its well-established functions as a nuclear transcription factor, transcription-independent mechanisms have been found in recent years by which p53 can promote apoptosis in the cytosol and mitochondria [48]. One of these transcription-independent mechanisms involves the physical interaction between the p53 and Bcl-2 family proteins [49]. The Bcl-2 family contains both anti-apoptotic members and pro-apoptotic members, which regulate apoptosis and tumorigenesis by their complex interaction networks [50, 51]. Although the Bcl-2 related proteins have received the most attention from researchers, other non-Bcl-2-like proteins have also been identified as regulators of apoptosis. The best example is the tumor-suppressor gene p53. In addition to the well-known nuclear and transcriptional roles of p53, there is new and mounting evidence which suggests that p53 may act via mitochondrial mechanisms to induce apoptosis [49, 52]. In at least some cell types, p53 induces apoptosis via interaction with the pro-apoptotic Bcl-2 family member Bim, which is associated with the outer mitochondrial membrane [50]. Furthermore, transcription of the Bax gene in some human cells is directly activated by p53-binding sites in the regulatory region of the gene [49]. However, p53 can directly target the mitochondria and induce mitochondrial disruption [53, 54].

In this study, we first showed that ST kinase could induce cell death in fish cells through a mitochondria/caspase-mediated death pathway. Then we observed that kinase overexpression induced the expression of p53 and the pro-apoptotic protein Bax at 48 hpt (Fig. 5), and the downregulation of Bcl-2 (Fig. 6). This pattern was

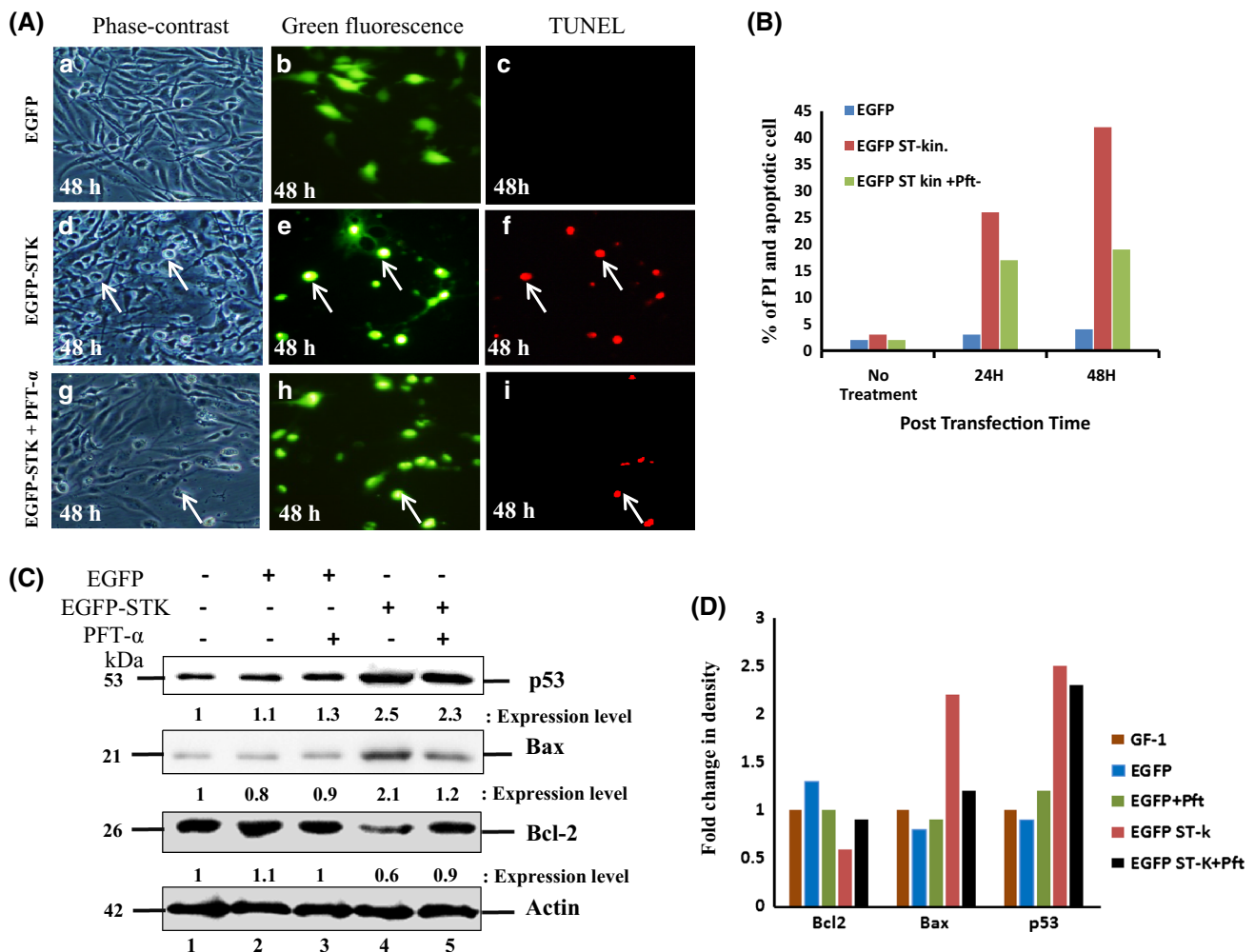
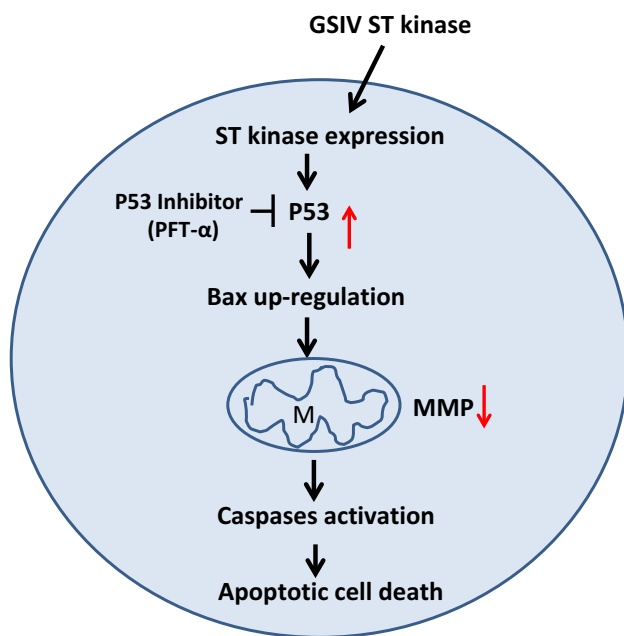


Fig. 9 Inactivation of p53 function by specific inhibitor PFT- α can reduce pro-apoptotic gene Bax expression in ST kinase transfected cells. **A** Treatment of PFT- α can reduce the ST kinase-induced apoptotic rate in GF-1 cells at 0, 24 and 48 h PT, by TUNEL assay. The cells were pre-treated with 20 μ M PFT- α for 4 h or left without treatment, and then treated by transfection with vector control (pEGFP) and ST kinase-contained plasmid (pEGFP-ST kinase) at 48 hpt. The cells are shown for the vector control group (**A**, *a–c*), the ST kinase transfected group (**A**, *d–f*) and the PFT- α treated plus ST kinase transfected groups (**A**, *g–i*), in which the TUNEL-positive cells are indicated by arrows. **B** The PFT- α treatment-caused reductions in ST kinase-induced apoptosis in GF-1 cells were counted at 0, 24 h and 48 hpt. The number of TUNEL-positive cells in each 200 cell

sample were assessed in three individual experiments. Each point represents the mean TUNEL-positive cells of three independent experiments \pm the standard error of the mean (SEM). The data were analyzed using either paired or unpaired Student's *t* tests, as appropriate. Statistical significance was defined as *p* values <0.05 . **C** Identification of PFT- α treatment can reduce Bax upregulation and Bcl-2 downregulation with ST kinase transfection in GF-1 cells at 48 hpt as shown by Western blot analysis. Lane 1 displays cells without transfection; lane 2 displays cells transfected with pEGFP; lane 3 displays pEGFP plus PFT- α treatment; lane 4 displays pEGFP-ST kinase; lane 5 displays pEGFP-ST kinase plus PFT- α treatment; lane 7 contains the control MCF-7 cell lysate. **D** Quantification of protein expression level by Image J software, from **C**

correlated with the loss of MMP during GSIV infection, but not with upregulation of Bak (data not shown). Furthermore, PFT- α [55], an inhibitor that inactivates p53, was found to not only inhibit the Bax upregulation, but also to reduce ST kinase-induced apoptosis, which meant that p53 was a upstream factor for regulating the downstreaming of Bax gene expression during ST kinase expression in GF-1 cells, which may act as modulated targets.

Summary (Fig. 10): Taken altogether, our data suggest that overexpression of the early expression gene ST kinase can induce cell death via various forms of apoptosis, such as mitochondria disruption or caspases -9 and -3 activations. Then the SK kinase-induced cell death may upregulate the p53 and Bax (pro-apoptotic gene) at 24 h and 48 hpt. Furthermore, it was found that p53 inactivation (by its specific inhibitor PFT- α) could also reduce downstream gene Bax expression and avert cell death.



The GSIV ST kinase induces apoptotic cell death cascade in fish cells

Fig. 10 The hypothesis that GSIV ST kinase induces apoptotic cell death cascade in fish cells. The novel ST kinase expressions can upregulate either p53 or Bax for inducing apoptotic cell death. This STK-induced death pathway is also correlated to downstream mitochondrial disruption and caspase activation in GF-1 cells. Interestingly, the STK-induced Bax-mediated cell death signaling was modulated by the p53 specific inhibitor PFT- α , which affected p53 inactivation for averting fish cell death

Acknowledgments The authors are grateful to Dr. S. C. Shi (Institute of Zoology and Department of Life Science, National Taiwan University, 1, Sec., 4, Roosevelt Rd., Taipei 10617, Taiwan, ROC) for providing the GF-1 cell line and to Dr. C. M. Wen (Department of Life Sciences, National University of Kaohsiung, Kaohsiung 811, Taiwan, ROC) for providing the GSIV K1 strain. This research was supported by Grants (NSC-99-2321-B-006-010-MY3; MOST 104-2313-B-006-003) awarded to Dr. Jaiinn-Ruey Hong from the National Science Council, Taiwan, Republic of China.

References

- Clarke P, Tyler KL (2009) Apoptosis in animal models of virus induced disease. *Nat Rev Microbiol* 7:144–155
- Gray MJ, Miller DL, Hoverman JT (2009) Ecology and pathology of amphibian ranaviruses. *Dis Aquat Org* 87:243–266
- Williams T, Barbosa SV, Chinchar VG (2005) A decade of advances in iridovirus research. *Adv Virus Res* 65:173–248
- Jancovich JK, Chinchar VG, Hyatt A, Miyazaki T, Williams T (2011) Family iridoviridae. In: King AMQ, Lefkowitz E, Adams MJ, Carstens EB (eds) *Virus taxonomy: 9th report of the international committee on taxonomy of viruses*. Elsevier, San Diego, pp 193–210
- Gibson-Kueh S, Netto P, Ngoh-Lim GH, Chang SF, Ho LL, Qin QW, Chua FHC, Ng ML, Ferguson HW (2003) The pathology of systemic iridoviral disease in fish. *J Comp Pathol* 129:111–119
- Huang XH, Huang YH, Ouyang ZL, Xu LX, Yan Y, Cui HC et al (2011) Singapore grouper iridovirus, a large DNA virus, induces non apoptotic cell death by a cell type dependent fashion and evokes ERK signaling. *Apoptosis* 16:831–845
- Pham PH, Lai YS, Lee FF, Bols NC, Chiou PP (2012) Differential viral propagation and induction of apoptosis by grouper iridovirus (GIV) in cell lines from three non-host species. *Virus Res* 167:16–25
- Hong JR, Lin TL, Hsu YL, Wu JL (1998) Apoptosis proceeds necrosis of fish cell line by infectious pancreatic necrosis virus. *Virology* 250:76–84
- Chao CB, Yang SC, Tsai HY, Chen CY, Lin CS, Huang HT (2002) A nested PCR for the detection of grouper iridovirus in Taiwan (TGIV) in cultured hybrid grouper, giant seaperch, and largemouth bass. *J Aquat Anim Heal* 14:104–113
- Wang CS, Shih HH, Ku CC, Chen SN (2003) Studies on epizootic iridovirus infection among red sea bream, *Pagrus major* (Temminck and Schlegel), cultured in Taiwan. *J Fish Dis* 26:127–133
- Wen CM, Lee CW, Wang CS, Cheng YH, Huang HY (2008) Development of two cell lines from *Epinephelus coioides* brain tissue for characterization of betanodavirus and megalocytivirus infectivity and propagation. *Aquaculture* 278:14–21
- Chen XY, Wen CM, Wu JL, Su YC, Hong JR (2015) Giant seaperch iridovirus infection upregulates Bax and Bak expression, leading to apoptotic death of fish cells. *Fish Shellfish Immunol* 45:848–857
- Chen XY, Wen CW, Wu JL, Su YC, Hong JR (2016) Giant seaperch iridovirus induces mitochondria-mediated cell death that is suppressed by bongkreikic acid and cycloheximide in fish cell line. *Virus Res* 213:37–75
- Labbe K, Saleh M (2008) Cell death in the host response to infection. *Cell Death Differ* 15:1339–1349
- Chen SP, Wu JL, Su YC, Hong JR (2007) Anti-Bcl-2 family members, zfBcl-xL and zfMcl-1a, prevent cytochrome c release from cells undergoing betanodavirus induced secondary necrotic cell death. *Apoptosis* 12:1043–1060
- Hong JR, Huang LJ, Wu JL (2005) Fish birnavirus induces apoptotic through activated caspases 8 and 3 in zebrafish cell line. *J Fish Dis* 28:1–8
- Hong JR, Gong HY, Wu JL (2002) VP5, a novel anti-apoptosis of Bcl-2 family member that up-regulates the Mcl-1 and limit-regulates the viral proteins expression. *Virology* 295:217–229
- Wyllie AH, Kerr JFR, Currie AR (1980) Cell death: the significance of apoptosis. *Int Rev Cytol* 68:251–306
- Kumar S (2006) Caspase function in programmed cell death. *Cell Death Differ* 14:32–43
- Ameisen JC (2002) On the origin, evolution, and nature of programmed cell death: a timeline of four billion years. *Cell Death Differ* 9:367–393
- Benedict CA, Norris PS, Ware CF (2002) To kill or be killed: viral evasion of apoptosis. *Nat Immunol* 3:1013–1018
- Vanlandschoot P, Leroux-Roels G (2003) Viral apoptotic mimicry: an immune evasion strategy developed by the hepatitis B virus? *Trends Immunol* 24:144–147
- Levine AJ (1997) P53, the cellular gatekeeper for growth and division. *Cell* 88:323–331
- Nagata S (1997) Apoptosis by death factor. *Cell* 88:355–365
- White E (1996) Life, death, and the pursuit of apoptosis. *Genes Dev* 10:1–15
- Chen PC, Wu JL, Her GM, Hong JR (2010) Aquatic birnavirus induces necrotic cell death via mitochondria-mediated caspases pathway that is inhibited by bongkreikic acid. *Fish Shellfish Immunol* 28:344–353

27. Ferri KF, Kroemer G (2001) Organelle-specific initiation of cell death pathways. *Nat Cell Biol* 3:E255–E263
28. Wu HC, Wu JL, Chu HL, Su YC, Hong JR (2010) RGNNV induces mitochondria mediated cell death via newly synthesized protein dependent pathway in fish cells. *Fish Shellfish Immunol* 29:451–463
29. Hong JR (2013) Betanodavirus: mitochondrial disruption and necrotic cell death. *World J Virol* 2(1):1–5
30. Chen MC, Gong HY, Cheng CY, Wang JP, Hong JR, Wu JL (2001) Cloning and characterization of zfBLP1, zfBcl-xL homologue from the zebrafish, *Danio rerio*. *Biochim Biophys Acta* 1519:127–133
31. Zamzami N, Kroemer G (2001) The mitochondrion in apoptosis: how Pandora's box opens. *Nat Rev Mol Cell Biol* 2:67–71
32. Hong JR, Wu JL (2002) Induction of apoptotic death in cells via bad gene expression by infectious pancreatic necrosis virus infection. *Cell Death Differ* 9:113–124
33. Dobos P, Hill B, Hallett R, Kells D, Becht H, Teninges D (1979) Biophysical and biochemical characterization of five animal viruses with bi-segmented double stranded RNA genomes. *J Virol* 32:593–605
34. Kurita J, Nakajima K (2012) Review: megalocytivirus. *Viruses* 4:521–538
35. Subramaniam K, Shariff M, Omar AR, Hair-Bejo M (2012) Megalocytivirus infection in fish. *Rev Aquac* 4:221–233
36. Hong JR, Lin TL, Yang JY, Hsu YL, Wu JL (1999) Dynamics of non-typical apoptotic morphological changes visualized by green fluorescent protein in living cells with infectious pancreatic necrosis virus infection. *J Virol* 73:5056–5063
37. Yoshida M (2001) Multiple viral strategies of HTLV-1 for dysregulation of cell growth control. *Annu Rev Immunol* 19:475–497
38. Seet BT, Hohnston JB, Brunetti CR, Barrett JW, Everett H, Cameron C, Sypula J, Nazarian SH, Lucas A, McFadden G (2003) Poxviruses and immune evasion. *Annu Rev Immunol* 21:377–423
39. Evertt H, McFadden G (1999) Apoptosis: an innate immune response to virus infection. *Trends Microbiol* 7:160–165
40. Chen SP, Yang HL, Her GH, Lin HY, Jeng MF, Wu JL, Hong JR (2006) NNV induces phosphatidylserine exposure and loss of mitochondrial membrane potential in secondary necrotic cells, both of which are blocked by bongkreikic acid. *Virology* 347:379–391
41. Wu HC, Chiu CS, Wu JL, Chen MC, Li MW, Hong JR (2008) Zebrafish anti-apoptotic protein zfBcl-xL can block betanodavirus protein α -induced mitochondria-mediated apoptotic cell death. *Fish Shellfish Immunol* 45:1146–1152
42. Su YC, Hong JR (2010) Betanodavirus B2 causes ATP depletion-induced cell death via mitochondrial targeting and complex II inhibition in vitro and in vivo. *J Biol Chem* 285:39801–39810
43. Su YC, Chiu HW, Hung JC, Hong JR (2014) Beta-nodavirus B2 protein induces hydrogen peroxide production, leading to Drp1-recruited mitochondrial fragmentation and cell death via mitochondrial targeting. *Apoptosis* 19:1457–1470
44. Zander K, Sherman M, Tessmer U, Bruns K, Wray V, Prechtel A, Schubert E, Henklein P, Luban J, Neidleman J, Greene WC, Schubert U (2003) Cyclophilin A interacts with HIV-1 Vpr and is required for its functional expression. *J Biol Chem* 278:43202–43213
45. Takada S, Shirakata Y, Kaneniwa N, Koike K (1999) Association of hepatitis B virus X protein with mitochondria causes mitochondrial aggregation at the nuclear periphery, leading to cell death. *Oncogene* 18:6965–6973
46. Riley T, Sontag E, Chen P, Levine A (2008) Transcriptional control of human p53-regulated genes. *Nat Rev Mol Cell Biol* 9:402–412
47. Vousden KH, Prives C (2009) Blinded by the light: the growing complexity of p53. *Cell* 137:413–431
48. Speidel D (2010) Transcription-independent p53 apoptosis: an alternative route to death. *Trends Cell Biol* 20:14–24
49. Chipuk JE, Kuwana T, Bouchier-Hayes L, Droin NM, Newmeyer DD, Schuler M et al (2004) Direct activation of Bax by p53 mediates mitochondrial membrane permeabilization and apoptosis. *Science* 303:1010–1014
50. Han J, Goldstein LA, Hou W, Gastman BR, Rabinowich H (2010) Regulation of mitochondrial apoptotic events by p53-mediated disruption of complexes between anti-apoptotic Bcl-2 members and Bim. *J Biol Chem* 285:22473–22483
51. Geng Y, Walls KC, Ghosh AP, Akhtar RS, Klocke BJ, Roth KA (2009) Cytoplasmic p53 and activated Bax regulate p53-dependent, transcription-independent neural precursor cell apoptosis. *J Histochem Cytochem* 58:265–275
52. Marchenko ND, Zaika A, Moll UM (2000) Death signal induced localization of p53 protein to mitochondria: a potential role in apoptotic signaling. *J Biol Chem* 275:16202–16212
53. Arima Y, Nitta M, Kuninaka S, Zhang D, Fujiwara T, Taya Y et al (2005) Transcriptional blockade induces p53-dependent apoptosis associated with translocation of p53 to mitochondria. *J Biol Chem* 280:19166–19176
54. Mossalam M, Matissek KJ, Okal A, Constance JE, Lim CS (2012) Direct induction of apoptosis using an optimal mitochondrially targeted p53. *Mol Pharm* 9:1449–1458
55. Komarov PG, Komarova EA, Kondratov RV, Christov-Tselkov K, Coon JS, Chernov MV, Gudkov AV (1999) A chemical inhibitor of p53 that protects mice from the side-effects of cancer therapy. *Science* 285(5434):1733–1737